Progress in Neurobiology 210 (2022) 102215

Contents lists available at ScienceDirect

Progress in Neurobiology

journal homepage: www.elsevier.com/locate/pneurobio

Original Research Article

Injury to thalamocortical projections following traumatic brain injury results in attractor dynamics for cortical networks

Sima Mofakham [a,b,*], Yuhao Liu [b], Asher Hensley [b], Jordan R. Saadon [a], Theresa Gammel [a], Megan E. Cosgrove [a], Joseph Adachi [a], Selma Mohammad [a], Chuan Huang [c,d], Petar M. Djurić [b], Charles B. Mikell [a]

[a] Department of Neurosurgery, Stony Brook University Hospital, Stony Brook, NY, USA
[b] Department of Electrical and Computer Engineering, Stony Brook University, Stony Brook, NY, USA
[c] Department of Radiology, Stony Brook University Hospital, Stony Brook, NY, USA
[d] Department of Psychiatry, Stony Brook University Hospital, Stony Brook, NY, USA

ARTICLE INFO

Keywords:
Traumatic brain injury (TBI)
Recovery of consciousness
Thalamocortical loop
Phase space reconstruction
Gaussian processes
Yule-Simon processes

ABSTRACT

Major theories of consciousness predict that complex electroencephalographic (EEG) activity is required for consciousness, yet it is not clear how such activity arises in the corticothalamic system. The thalamus is well-known to control cortical excitability via interlaminar projections, but whether thalamic input is needed for complexity is not known. We hypothesized that the thalamus facilitates complex activity by adjusting synaptic connectivity, thereby increasing the availability of different configurations of cortical neurons (cortical "states"), as well as the probability of state transitions. To test this hypothesis, we characterized EEG activity from prefrontal cortex (PFC) in traumatic brain injury (TBI) patients with and without injuries to thalamocortical projections, measured with diffusion tensor imaging (DTI). We found that injury to thalamic projections (especially from the mediodorsal thalamus) was strongly associated with unconsciousness and delta-band EEG activity. Using advanced signal processing techniques, we found that lack of thalamic input led to 1.) attractor dynamics for cortical networks with a tendency to visit the same states, 2.) a reduced repertoire of possible states, and 3.) high predictability of transitions between states. These results imply that complex PFC activity associated with consciousness depends on thalamic input. Our model implies that restoration of cortical connectivity is a critical function of the thalamus after brain injury. We draw a critical connection between thalamic input and complex cortical activity associated with consciousness.

1. Introduction

The return of consciousness following severe traumatic brain injury (TBI) is uncertain and hard to predict (Winans et al., 2019). Several lines of research including neuroimaging, behavioral analysis, and electrophysiological recordings have been focused on detecting early signs of recovery of consciousness following TBI (Synek, 1988; Casali et al., 2013; Sitt et al., 2014; Zhao et al., 2021; Wang et al., 2021; Cosgrove et al., 2022). The correlation between complex electroencephalography (EEG) activity and consciousness was originally noted by Hans Berger (Berger, 1929), and has been replicated many times since (Casali et al., 2013; Sitt et al., 2014; King et al., 2013). However, it is not clear how this complex cortical activity arises. The cortex switches between synchronized and desynchronized modes of activity based on wakefulness and attentional demands; these states depend on whether thalamic neurons, which project to the cortex, are in phasic or tonic firing modes, respectively (Glenn and Steriade, 1982; Domich et al., 1986; Llinás and Steriade, 2006). The oscillations that characterize these states are well-described (Berger, 1929); however, it is not clear what consequences synchronization and desynchronization have for cortical function. Desynchronized activity is more complex, and thus more capable of encoding information, which accords with a key prediction of Integrated Information Theory, an influential theory of consciousness (Koch et al., 2016).

Desynchronized activity can vary with task state and level of arousal, and it is not clear how it arises mechanistically (Pfurtscheller and Aranibar, 1977). Dynamic adjustment of synaptic gain is a likely mechanistic contributor to desynchronization; when synaptic gain is adjusted,

* Corresponding author at: Department of Neurological Surgery, Stony Brook University Hospital, 101 Nicolls Road, Stony Brook, NY, 11794, USA.
E-mail address: Sima.Mofakham@stonybrookmedicine.edu (S. Mofakham).

https://doi.org/10.1016/j.pneurobio.2022.102215
Received 14 October 2021; Received in revised form 29 December 2021; Accepted 3 January 2022
Available online 4 January 2022

it facilitates transitions between chaotic activity and dynamic attractor states used for high-reliability information transmission (Laje and Buonomano, 2013). Recent reports have highlighted the role of the mediodorsal thalamus in adjusting synaptic gain in the prefrontal cortex to facilitate neuronal ensemble formation in response to behavioral demands (Schmitt et al., 2017). Building on these findings, our group recently demonstrated that withdrawal of gain adjustment by the thalamus results in highly predictable, attractor-like dynamics (Mofakham et al., 2021). Therefore, we hypothesized that lack of thalamic input strongly constrains the flexibility of the cortex, and only allows it to adopt a small number of possible states. This hypothesis leads to the prediction that the thalamus is a key driver of flexibility in the cortex, and patients who lack thalamic input will be unconscious, but partial thalamic injuries will allow for partial consciousness.

In the present report, we tested this hypothesis by evaluating unconscious TBI patients with diffusion tensor imaging (DTI) and EEG recordings. We utilized machine learning and dynamical systems tools to uncover the underlying phase space governing the cortical network dynamics and its temporal evolution as a function of thalamic integrity. We found that return to consciousness (RTC) was associated with preserved thalamic projections, which support complex and unpredictable cortical dynamics.

2. Methods

2.1. Ethics statement

This study was a retrospective study that was approved by the Stony Brook University Hospital (SBUH) Committee on Research Involving Human Subjects (CORIHS) with a waiver of consent (IRB2019-00464).

2.2. Study subjects

In this study, we identified fifteen TBI patients (age $\geq$ 18) with an initial Glasgow Coma Scale (GCS) $<$ 8 and analyzable DTI and EEG recordings. The patient characteristics are listed in Table 1. We identified the date that patients followed a simple verbal command for the first time after injury. We stratified patients in two ways: (1) clinical outcome and (2) the thalamo-prefrontal structural integrity. *Favorable* outcome was defined as the ability to follow commands within two months of injury and a Glasgow Outcome Score (GOS) of more than two (patient is not dead or in persistent vegetative state) at discharge. The structural integrity was measured using FA values adjusted for sex and age.

2.3. EEG recordings

We recorded scalp EEG leads in an 18-contact standard 10–20 system EEG with a sampling frequency of 256 Hz. For each patient, we identified a minimum of forty minutes of resting data with minimal sedation and artifact. Then, we used custom MATLAB codes to analyze these signals. Before analysis, we preprocessed these EEG recordings by screening for artifact, mean subtraction, bipolar re-referencing, and bandpass filtering (0.5−30 Hz).

2.4. Frequency analysis

We calculated the power spectral density (PSD) using Welch's overlapped segment averaging estimator with a Hamming window and 50% overlap. Frequency analysis was performed over the 0.5−30 Hz range. In order to quantify and compare power spectra across patients, we normalized the area under the curve of the power spectrum (within the range of 0.5–30 Hz) for each patient (Fig. 1). Then, we compared the power at theta (4−8 Hz), alpha (8−12 Hz), and beta (12−30 Hz) bands to the delta band power shown in Fig. 1C.

2.5. Lempel-Ziv complexity analysis

We utilized the Lempel-Ziv complexity measure (LZ), a widely used measure of complexity in biological sciences, to quantify EEG recordings. The LZ metric assesses the complexity of the signal by the number of unique patterns found in that signal. Before the LZ complexity analysis, the signals were band-pass filtered (0.5–10 Hz, 4th order Butterworth notch filter) and converted to one-dimensional binary signals using the median method. We normalized the output of the LZ analysis to the length of the sequence.

2.6. Phase space reconstruction

As described by Takens's theorem, delay embedding methodology provides a framework for reconstructing the phase space of the underlying global dynamics of a system using only one of its variables. For instance, a single EEG channel recording (we used the Fz-Cz channel) provides information about the global dynamics of the cortical networks. Prior to the delay embedding analysis, we preprocessed the scalp EEG data by subtracting the mean, bandpass filtering (0.5−20 Hz), and bipolar preprocessing (subtracting Cz from the Fz channel). Then, we used an artifact-free ten minutes of resting data from the Fz-Cz channel to reconstruct the underlying attractor of cortical recordings in the phase space for our fifteen TBI patients.

The delay embedding method requires an estimation of two parameters: (1) the embedding dimension (m) and (2) the time delay (τ). Here, we used autocorrelation to estimate an appropriate time delay. In particular, the time that autocorrelation drops below zero determines the appropriate delay period. MATLAB's built-in

Table 1
Patient characteristics.

Patient	(1) Gender	(2) Age	(3) GCS at EEG	(4) Days to Follow Commands	(5) GOS Discharge	(6) Average FA Values for Whole Thalamus	(7) Minimum Sedation
1	M	84	7	3	1	0.035	No sedation
2	M	63	6	24	3	0.03	Fentanyl 50 mcg q1h
3	F	25	7	11	3	0.027	No sedation
4	M	30	7	3	4	0.025	Fentanyl 25 mcg q2h
5	M	70	7	15	4	0.025	Fentanyl 25 mcg q2h
6	M	72	7	10	3	0.013	No sedation
7	M	84	7	53	2	0.012	Fentanyl 25 mcg x1
8	F	44	7	6	3	0.01	Fentanyl 25 mcg q2h
9	M	57	3	Never	1	−0.003	Oxycodone 5 mg
10	M	24	3	12	2	−0.013	Precedex 0.3 mcg/kg/hr
11	M	76	3	Never	1	−0.017	No sedation
12	F	34	6	127	2	−0.022	Fentanyl 25 mcg q2h
13	M	43	6	178	3	−0.032	Fentanyl 25 mcg q2h
14	F	74	3	Never	1	−0.042	Fentanyl 50 mcg q1h
15	M	27	7	144	3	−0.095	Fentanyl 50 mcg q2h

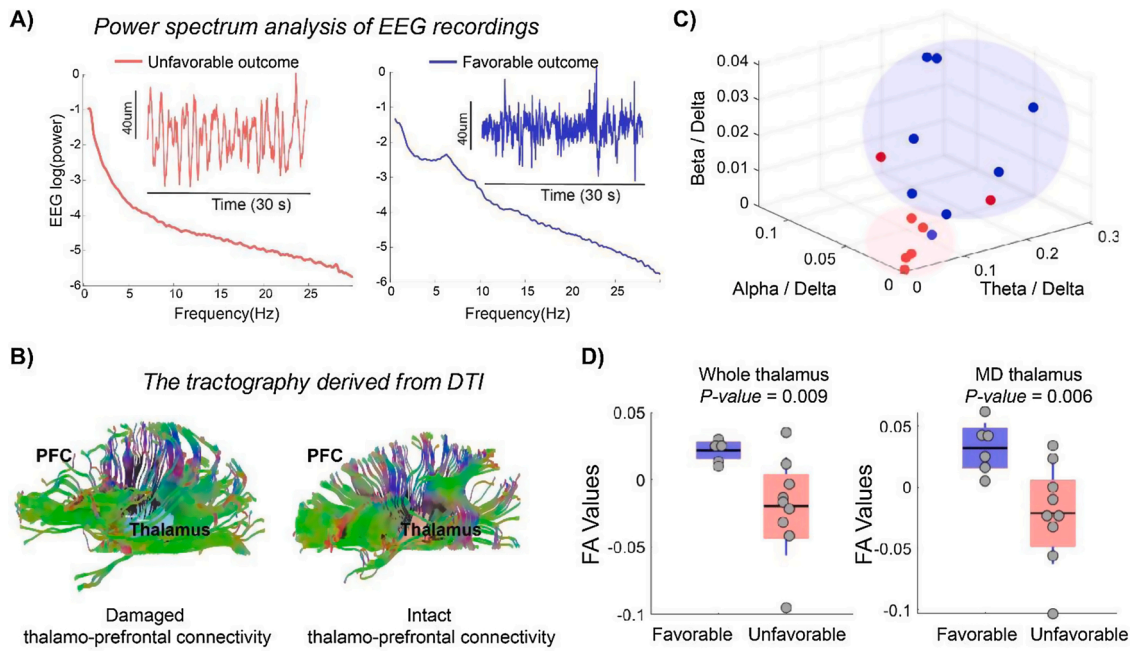

Fig. 1. EEG signatures of thalamic injury. (A) The EEG recording and power spectrum density for two patients with favorable and unfavorable outcomes are plotted in blue and red. Power spectrum density was calculated for one-minute windows and averaged across 60 windows with 30 s of overlap. **(B)** Tractography derived from DTI imaging for the two patients in panel (**A**), which shows intact thalamic projections to PFC (right) in the patient with a favorable outcome and loss of tracts (left) for the patient with unfavorable outcome. (**C**) Ratios of EEG power at theta, alpha, and beta were calculated and plotted for each of the fifteen patients in this study. These measurements are color-coded based on the integrity of thalamic tracts projecting to mPFC, DLPFC, and ACC measured using FA values (blue dots represent patients with intact projections and red dots are those with damaged projections). Shaded blue and red circles are included to visually display regions of the plot associated with mostly poor (red) and intact (blue) thalamo-prefrontal connectivity. The *kmeans* method (using MATLAB) detected the centroids associated with two clusters (low frequency and high frequency) and the Euclidian distance to the higher frequency centroid was significantly lower for patients with intact thalamocortical projections compared to the patients with injuries to their thalamocortical projections (*P-value* = 0.01). In general, impaired projections were associated with low beta and variable amounts of alpha and theta activity. **(D)** Tractography results with whole thalamus (left) and MD (right) as seed regions reveal a direct correlation between the integrity of thalamus-PFC connectivity and patient outcomes. Note that the mean FA values are age and sex corrected.

phaseSpaceReconstruction function was employed to calculate the sufficient embedding dimension using the false nearest neighbors (FNN) algorithm. The *phaseSpaceReconstruction* function reconstructs the phase space using these two parameters.

2.7. Recurrence plots and recurrence quantification analysis

We utilized recurrence plots and Recurrence Quantification Analysis (RQA) to visualize and quantify temporal developments of the *m*-dimensional reconstructed EEG recordings' phase space. Here, we used RQA to explore the temporal statistics of state recurrence in the reconstructed phase space.

Recurrence plots were formed by calculating the Euclidean distance of each state, in the reconstructed *m*-dimensional phase space, to any other states. When the state trajectory visits a neighborhood of a previously visited state, the Euclidean distance between the current state and the previously visited state drops under a certain threshold, and RQA marks this time as a state recurrence ($R_{ij}<$ threshold). This state recurrence is plotted as a single point in the recurrence plot.

We divided the ten-minute reconstructed phase space into 58 twenty second windows (with a ten-second overlap). Next, we formed the recurrence plots for each time window, followed by RQA quantification that included recurrence rates, determinism, and trapping time. Finally, we compared the RP statistics to estimate determinism and trapping time. For consistency, we kept the recurrence rate fixed at 10% across patients. Determinism was calculated based on the fraction of recurrence points that formed parallel lines to the main diagonal. While the fraction of points that formed the vertical lines to the total recurrence is a measure of the trapping time.

2.8. Gaussian process prediction

We utilized our advanced, house-developed machine learning tool called Sequential Ensemble Gaussian Process, an online Bayesian model, to assess the predictability of these EEG signals (Lu et al., 2020). First, we downsampled (by 5), normalized, and bandpass filtered (Butterworth, 0.5−30 Hz) forty minute EEG recordings from Fz-Cz channels. Next, we divided the signal into twelve segments of 10,100 decimated samples—the first 10,000 as the training set and the remaining 100 samples for testing. Then, we used the median relative absolute error (MdRAE) to compare the one-step forward predictability of signals across patients and the MdRAE for each segment (Fig. 2E, F, and Supplementary Fig. 4). After training the first 10,000 samples, we also examined the predictability of these signals over the following 100 samples step-by-step without observing those values. The procedure is demonstrated in Supplementary Fig. 1.

2.9. Yule–Simon processes

We also applied a Yule-Simon process generative model to the EEG time series (the Fz-Cz channel in particular) to identify the latent structure within the data and study its statistical properties. Specifically, the Yule-Simon generative model provides a Bayesian nonparametric prior over partitions of a sequential set of measurements. Such a prior acts as a flexible model that explains how the data we observe was created. Once we observe the EEG time-series data, the objective then becomes to invert the generative process and infer the latent model variables conditioned on the measurements. We can think of this as an inverse problem where we observe the output of a probabilistic system and need to find the posterior distribution of the system given the

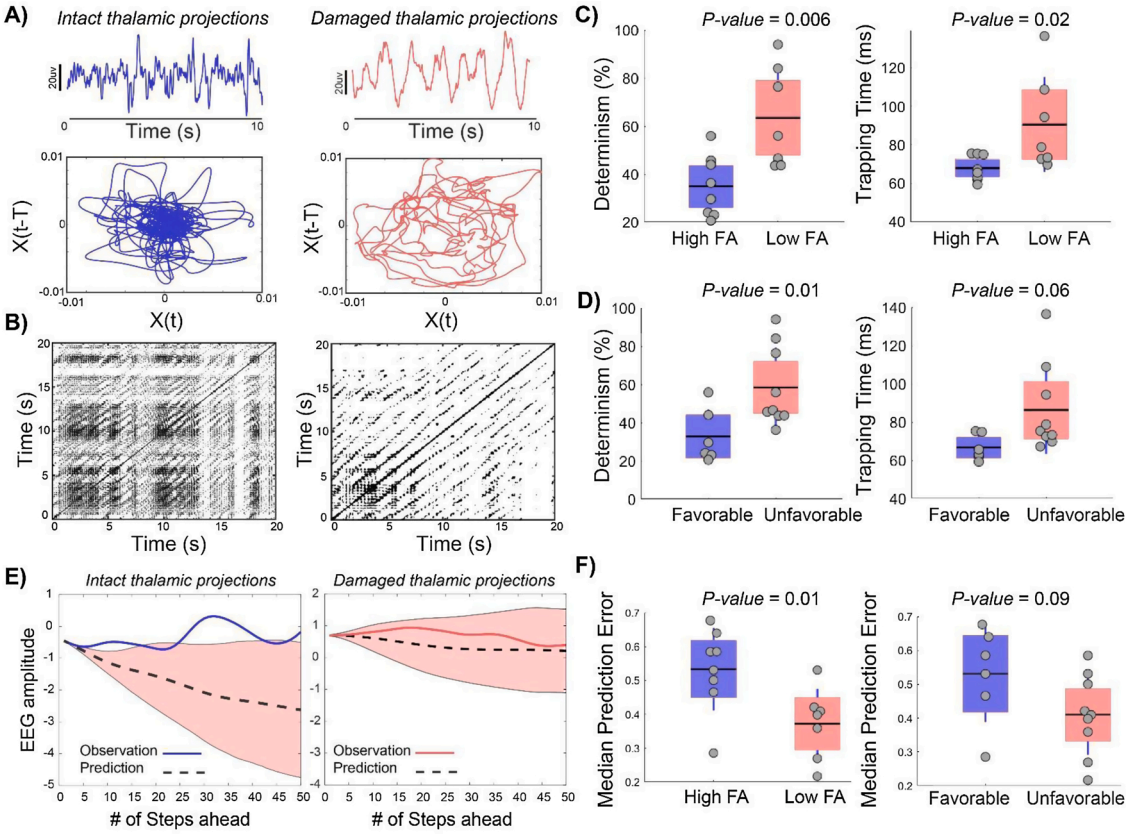

Fig. 2. Reconstruction of the underlying phase space of EEG recordings reveals high levels of determinism (predictability) for patients with severe injuries to their thalamocortical projections. (A) shows the phase space reconstruction of EEG recordings for two patients with preserved (left, in blue) and poor (right, in red) integrity of thalamocortical projections. When thalamic projections are intact (blue) the phase space of cortical dynamics is complex. Still, when thalamic projections are damaged, the reconstructed phase space of cortical networks is structured, the number of visited states is limited, and the trajectory of visiting states is predictable. (**B)** The recurrence plots of the reconstructed phase space show these differences more clearly as it is based on all dimensions (not only the first two dimensions) of the reconstructed phase space. A repeated trajectory of visited states on the recurrence plots manifests itself as a diagonal line parallel to the main diagonal (black line). The degree of determinism of a dynamical system can be estimated by the percentage of recurrence states on the diagonal lines parallel to the main diagonal to the total recurrence of the system. For the patient shown in panel A with thalamic injury (red), the recurrence plots look ordered with long lines parallel to the main diagonal. (**C, D)** Across all of our 15 patients, determinism significantly and negatively correlates with the integrity of thalamocortical projections measured with FA values (adjusted for sex and age) and patients' outcomes. (**E)** Two examples of EEG recordings from two TBI patients (Fz-Cz channel), one with intact (left) and the other one with injured (right) thalamo-prefrontal connections, are shown. The dashed lines are the predicted values with a shaded pink area for the confidence interval, and the solid lines are the actual observed values. A TBI patient with intact thalamo-prefrontal connectivity deflects the prediction confidence interval within a few steps. In contrast, the prediction trajectory in the patient with injured thalamo-prefrontal connectivity remains close to the predicted values. (**F)** One-step prediction measured with MdRAE remained higher over an extended period in patients with intact thalamo-frontal connectivity (left) and those with favorable outcomes (right).

output.

The Yule-Simon model is closely related to Polya urn processes, where preferential attachment plays a crucial role in how the state of the system evolves. Consider an urn with a single white ball and α black balls. The process proceeds by sequentially drawing balls from the urn. Similar to the Polya urn model, each time a white ball is drawn, the white ball is replaced in the urn with an additional white ball. When a black ball is drawn, the urn resets to its initial state with 1 white ball and α black balls—adding white balls to the urn after each white draw increases the probability of drawing additional white balls in the future. This is a preferential attachment effect that has the potential to generate highly long runs between system resets. As a result, the distribution of the waiting time between resets follows a power-law distribution where α controls the tail probabilities.

To apply the Yule-Simon model to EEG time series data, we use a latent Yule-Simon process as a state variable to control the dynamics of the observation sequence. To connect this idea to the above urn discussion, each time the system resets to its initial state (i.e., a black ball is drawn from the urn), the model parameters change. Between system resets, the model parameters remain constant. We can write this as the following hierarchical stochastic process:

$$
\begin{aligned}
s_t \left| n_t, \alpha \right. &\sim Bernoulli\left(\alpha (n_t + \alpha)^{-1}\right) \\
\lambda_k \left| a, b \right. &\sim Gamma(a, b) \\
y_t \left| \{\lambda\}, x_t \right. &\sim Normal\left(0, \lambda_{x_t}^{-1/2}\right) \\
x_t &= x_{t-1} + s_t \\
n_{t+1} &= (n_t + 1)^{1 - s_t}
\end{aligned}
$$

where the observation sequence, y_t, is modeled as a zero-mean Gaussian process with switching variance controlled by the latent state of the system, x_t. The Yule-Simon process is implemented as a Bernoulli process with feedback using the counter, n_t. Each time a white ball is drawn, s_t evaluates to 0, the counter, n_t, increments by one, and the state of the system, x_t, remains constant. Each time a black ball is drawn, s_t evaluates to one, the counter, n_t, resets to one, and the state of the system x_t, increments by one. Thus, the state variable x_t is a monotonic counter that increases by one each time the model parameters change. This variable is used as an index into the infinite set $\{\lambda\}$ which is randomly drawn from a Gamma prior. The implication of this is the number of latent states can be theoretically infinite. When applying the inference process,

the number of states (or sequence partitions) is primarily determined from the data itself, and the size of {λ} is increased dynamically to support the complexity of the given data set.

The inference was carried out by Markov Chain Monte Carlo (MCMC) sampling techniques. Here we give a high-level description of the process and refer the interested reader to (Hensley and Djurić, 2017) for more information on the specific sampling methods. Because the model posterior distribution is analytically intractable, we used MCMC sampling methods to draw random samples from the model posterior distribution. These samples can then be used to perform subsequent data analysis. MCMC works by simulating a Markov chain with the same stationary distribution as the posterior distribution we are interested in sampling from. Once the Markov chain converges, each step we take in the simulation will be a sample from the posterior distribution.

Our inference algorithm uses 3 MCMC samplers that have interleaved updates. The first sampler is a Gibbs sampler used to sample the state variable change points. This is the primary sampler used to partition the measurements into sets with similar statistics which are then used to update the set of precisions {λ} using the conjugacy properties of the Normal and Gamma distributions. The second sampler is another Gibbs sampler for the hyperparameter, a, which we model with a Gamma prior and follow the approach of Leisen (Leisen et al., 2017). The third sampler is a Metropolis-Hastings sampler for the hyperparameters, a, b, of the Gamma distribution which are modeled using the appropriate conjugate prior when both shape and rate parameters are unknown. To prepare the EEG data for the inference process, we began by applying the following transformation:

$$y_t = \log\left(z_t^2\right) - \log\left(z_{t-1}^2\right)$$

where z_t is the measured EEG time series data at time t and *log*() is the natural logarithm function. This operation is used extensively in finance to analyze the prices of market returns as it has several attractive properties. For this work, applying the "log-return" transformation provides a simple way to remove the mean process from the data as the generative model assumes the measurements are zero-mean. Additionally, this operation itself reveals interesting structures within the data which are not immediately obvious. As a final step before applying MCMC, the transformed time-series data for each patent was normalized by the standard deviation.

Next, the first 10,000 samples for each patient (Fs = 256 Hz) were divided into blocks of 1000 samples each of which is approximately 3.9 s long. The MCMC inference procedure was then applied to each 1000-sample block independently. Each Markov chain was run for 5000 steps with a 1000 step burn-in, although the Markov chain typically converged to the posterior much faster. The number of latent state transitions within each 1000-sample block was then estimated by taking the median over all the MCMC steps after burn-in. The median number of state transitions for each block for each patient was then used to study the differences between patients, with the main hypothesis being that patients with bad connectivity will have fewer state transitions on average than patients with good connectivity.

2.10. MRI and DTI acquisition

This study includes a secondary analysis of MRI scans; the detailed methodology for MRI and DTI analysis was reported in Cosgrove et al. (Cosgrove et al., 2022) In brief, MRI scans were obtained post-injury (mean: 11 days) to serve clinical purposes. All images were acquired on the same 3 T Siemens Trio MRI scanners. Structural images were collected via a 3D MPRAGE T1 weighted sequence with an isotropic voxel size of $1 \times 1 \times 1$ mm^3, and TE/ TR/ TI = 2.272/ 2300/ 915 ms, FA = 8. DTI images were collected with EPI sequence with a single b-value of 1000, slice thickness of 4 mm, TE/TR = 90/5400 ms, in-plane resolution of 2×2 mm^2, and 30 diffusion directions. The regions of interest (ROIs) were drawn manually using FMRIB software due to the severe brain distortion in this population of sTBI patients. Tracts between the whole thalamus and the mediodorsal thalamic nucleus (MD) and each of the combined prefrontal cortex regions were mapped using DSI Studio software (http://dsi-studio.labsolver.org). PFC regions included medial PFC (mPFC), anterior cingulate cortex (ACC), and dorsolateral PFC (DLPFC). Whole thalamus and MD ROIs were set as seed regions and PFC ROIs as end regions. The analysis in this paper is based on the whole thalamus seed, except as noted in Fig. 1. The tracking parameters were set to terminate at 10,000 tracts. Mean FA values of these tracts associated with mPFC, DLPFC, and ACC, after adjusting for sex and age, were calculated and compared to patient clinical outcomes and patterns of EEG activity. For all analyses, we assigned group membership to each patient based on whole thalamus to PFC connectivity (average of all three PFC subregions, see Results), which was similar to MD-PFC connectivity.

2.11. Statistics

We utilized a General Linear Model (GLM) to adjust FA values based on age and sex. We calculated a Student's *t*-test using SPSS to compare the mean FA values between the *favorable* and *unfavorable* outcomes. Additionally, the level of determinism and trapping time were categorized based on the integrity of the thalamo-prefrontal circuit (high FA versus low FA values) and the final cognitive outcome of these groups (*favorable* vs. *unfavorable* outcomes).

3. Results

We identified 15 severe TBI patients (9 males) who underwent MRI/ DTI scans as part of clinical care (Table 1). We reviewed their charts to determine the date when they returned to consciousness (defined as command following), and their outcome at discharge and six months following injury. We stratified patients in two ways: 1) clinical outcome and 2) the integrity of their thalamo-prefrontal circuit. Clinical outcome: Patients who were capable of following verbal commands within two months of injury and a Glasgow Outcome Score (GOS) of more than two at discharge were considered to have a *favorable* outcome, while those who expired or had prolonged unconsciousness (more than 60 days) or a GOS of less than three, were considered to have *unfavorable* outcomes. To classify the integrity of the thalamo-prefrontal circuit, we classified patients into two groups based on their thalamo-prefrontal circuit integrity measured by fractional anisotropy (FA), obtained from DTI analysis. After adjusting for sex and age, the residual FA values for thalamo-prefrontal connections were computed. We grouped patients into two groups: 1.) Low FA values, associated with poor integrity of thalamo-prefrontal connectivity and 2.) High FA values (FA > median), associated with preserved connectivity. The threshold used to group these patients was based on the median FA values of thalamo-prefrontal connectivity in a larger group of patients at our institution (Cosgrove et al., 2022). We previously reported the association of low FA values of thalamo-prefrontal connections with prolonged RTC (Cosgrove et al., 2022).

3.1. Thalamic input to the cortex correlates with complex, high-frequency PFC activity

Previous studies have linked simple, slow oscillations in EEG (particularly delta band) to poor outcomes in TBI patients (Synek, 1988; Forgacs et al., 2017). Fig. 1A shows a power spectrum analysis for two TBI patients with an *unfavorable* (red) and a *favorable* outcome (blue). We correlated power in canonical frequency bands to patient outcomes. The power spectrum of patients with *unfavorable* outcomes was dominated mainly by delta oscillations. In contrast, the power spectrum of those with *favorable* outcomes showed more prominent alpha and beta components. The *unfavorable* outcomes were generally associated with power law-type ($1/f$) EEG spectra consistent with previous findings

(Synek, 1988; Sitt et al., 2014). Delta band activity results from deafferentation of the cortex and thalamus, based on slice physiology (Timofeev et al., 2000) and human experiments (Forgacs et al., 2017). However, data on how the EEG power spectrum relates to the integrity of the thalamo-prefrontal circuit in the TBI setting is sparse. We examined this relationship by correlating the power spectrum with fractional anisotropy (FA), adjusted for sex and age, obtained from tractography of thalamic projections to the cortex (Fig. 1B & C). We found a subspace in the power spectrum coordinates associated with poor integrity of thalamic inputs to PFC (red sphere, that mostly includes red dots in Fig. 1C). A cluster of patients characterized by intact thalamic fibers had variable amounts of theta power but preserved alpha and beta power (blue region, that includes mostly blue dots in Fig. 1C). This clustering was less evident when we clustered by power spectrum and patient outcomes, without taking thalamic integrity into account.

In addition, the complexity analysis of the EEG signals showed a direct relationship with the integrity of the thalamo-prefrontal circuit and the complexity of the EEG signals (Supplementary Fig. 2), consistent with previous studies that linked the complexity of electrophysiological recordings to the return of goal-directed behavior and consciousness (Casali et al., 2013). Remarkably, the integrity of whole thalamus-PFC and MD-PFC connectivity correlated directly and significantly with patients' cognitive outcomes, measured by the ability to follow a verbal command (Fig. 1D).

3.2. Cortical dynamics are trapped in an attractor with predictable dynamics when deprived of thalamic input

To shed light on the role of the thalamus in shaping the cortical network dynamics, we used delay embedding methodology to reconstruct the underlying dynamical system of the cortical states, as represented in EEG recordings. These recordings are noisy, non-linear, and high-dimensional, making extraction of the underlying state dynamics challenging. Delay embedding methodology transforms a *one*-dimensional EEG time series into an *m*-dimensional phase space where each point represents a cortical state. The reconstructed phase space includes all the states available for the cortical networks represented in EEG and their temporal trajectory (Mofakham et al., 2021). Fig. 2A shows the reconstructed phase space of two sTBI patients with and without thalamic injury. We found that preserved thalamic projections were associated with complex, seemingly chaotic phase spaces (Fig. 2A, left panel). We observed that in comatose patients with impaired thalamic projections, the phase space is highly structured, resembling a low dimensional limit-cycle attractor (Fig. 2A, right panel). We have previously reported similar findings with intracranial recordings in TBI patients (Mofakham et al., 2021). These data are consistent with the hypothesis that thalamic input is required for rich cortical dynamics.

To quantify the extent to which thalamic injury results in recurrence of the attractor states, we utilized Poincaré recurrence plots (RP) analysis. A recurrence plot is a $t \times t$ matrix where t is time, and each point in the recurrence plot represents a time that a specific state in the phase space has been revisited (Fig. 2B; more examples are shown in Supplementary Fig. 3). Attractors are defined as dynamical features that cause the system dynamics to revisit a constrained set of states repeatedly (Strogatz, 2018). The parallel lines to the main diagonal in a RP represent a sequence of repeatedly visited states, measuring the system's determinism level. The vertical lines in a RP represent trapping time, the time that the trajectory is trapped at the revisiting state. Higher trapping time implies more constraints on the state transition. When we stratified the patients by low and high FA values of thalamic projections, we found that the group with low FA values (injuries extended to the thalamus) are associated with both higher levels of determinism of EEG activity and longer trapping time (Fig. 2C, $P = 0.006$ and 0.002, respectively).

We correlated the determinism in the trajectory of states to the cognitive outcomes of these patients (i.e. the ability to follow commands). We stratified the patients into two groups, *favorable* and *unfavorable* outcomes, where those with favorable outcomes were capable of following commands within two months of injury. Notably, we found: (1) a direct relationship between behavioral performance and integrity of thalamo-prefrontal connectivity (Fig. 1D), (2) an inverse relationship between determinism and the cognitive capacity to follow commands (Fig. 2D).

3.3. Highly predictable cortical dynamics when thalamic input is absent

William James noted that frogs with interrupted thalamocortical projections behave "like automata," whereas intact thalamocortical projections lead to unpredictable behavior (James, 1918). We thus sought to find out whether and to what extent this cortical attractor associated with loss of thalamic input is predictable. To see if EEG is predictable when thalamic input is absent, we utilized the state-of-the-art *Sequential Ensemble Gaussian Process* (Urteaga et al., 2015; Djurić et al., 2002) an online Bayesian methodology to model EEG recordings obtained from these patients. We analyzed segments of artifact-free EEG recordings. For each segment, we used the first 10,000 samples for training and the rest for prediction. We trained the model using the first 10,000 samples, whereas the last 100 samples were predicted. After training the first 10,000 samples, we performed (1) one-step prediction and (2) prediction of the following 100 samples based on the trained model from the 10,000 samples. We adopted the median relative absolute error (MdRAE) as a measure of predictive power. The predictive power for the one-step forward prediction was significantly higher in patients with injuries to their thalamo-prefrontal connections (P-value = 0.01, Fig. 2F). To obtain a more stable number and observe the change of predictive power with time, we divided the time series into twelve segments. The one-step prediction error measured by MdRAE remained consistently higher and more variable for patients with intact thalamo-prefrontal connections (Supplementary Fig. 4). Supplementary Fig. 4B shows the median of the MdRAE across patients with intact (in blue) and those with injured thalamo-prefrontal connections (in red) in each segment. Then, we examined the predictive power for 100 steps ahead. Supplementary Fig. 4A shows that for most of the patients with injuries to their thalamo-prefrontal connections, our metric could predict the evolution of their dynamics accurately with a narrow confidence interval instead of patients with intact thalamo-prefrontal connections.

3.4. The cortical attractor has a limited repertoire of possible states with a predictable trajectory

We hypothesized that thalamic input supports the ad-hoc assembly of new cortical states for ongoing cognitive activity. Thus, injuries to the thalamo-prefrontal inputs hinder the formation of spontaneous cortical ensembles and constrain the possible trajectories of the cortical states. Unconsciousness was previously associated with a decreased EEG microstate repertoire, especially in the alpha band (Fingelkurts et al., 2012). Our dynamical findings (see above) were consistent with this view, but we sought to 1.) quantify the number of states and state transitions and 2.) replicate our findings with a technique which does not rely on dynamical systems. Therefore, we quantified the number of possible states of EEG using a novel technique called Yule-Simon analysis. Yule-Simon processes are statistical processes closely related to urn processes that model latent state transitions. In brief, in the Yule-Simon processes a state is either maintained or transitioned to a new state, where the likelihood of a transition is inversely proportional to the time spent in the current state (a "rich get richer" process). With these simple assumptions, we can use Bayesian analysis to quantify the occupancy of the current state and the likelihood of a state transition. The transition probabilities are calculated by Markov Chain Monte Carlo (MCMC) sampling, which estimates the posterior distribution of the underlying Yule-Simon process. Fig. 3 shows the estimated Yule-Simon process for patients with and without thalamic injury. For technical reasons, it is

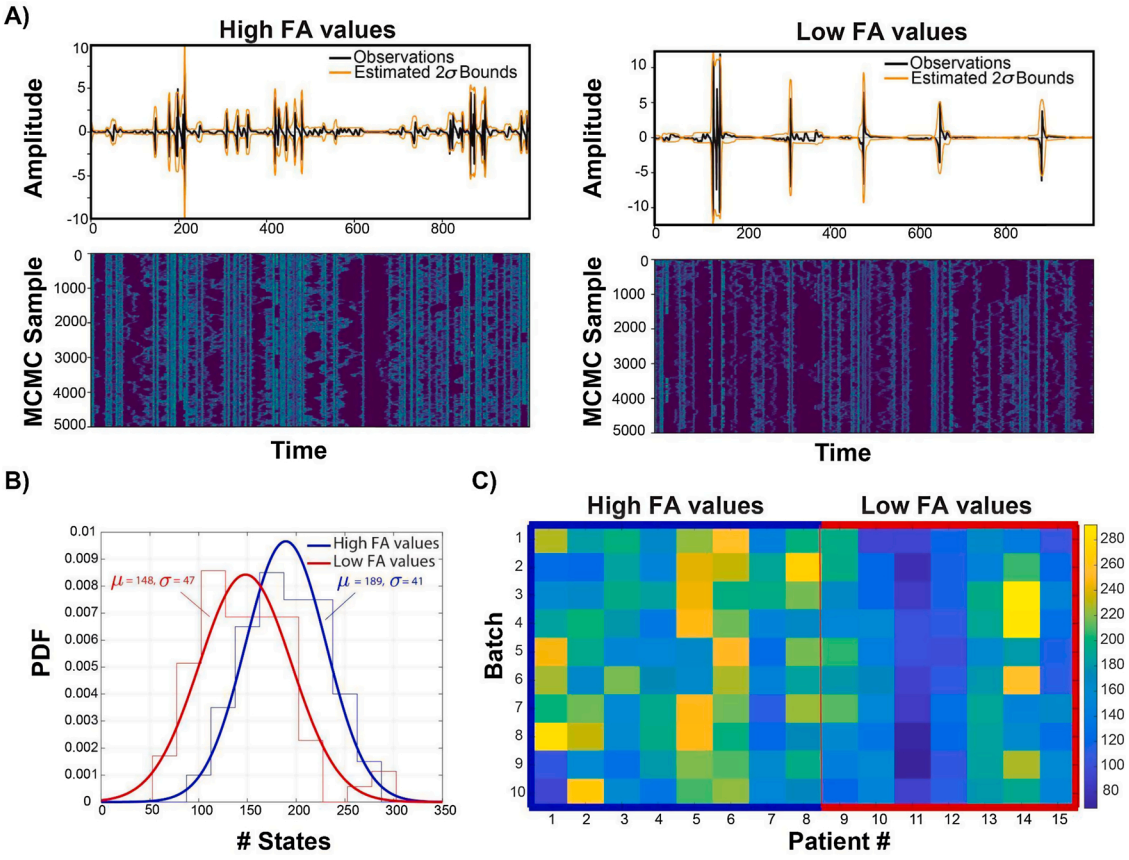

Fig. 3. Yule–Simon process reveals a limited number of available cortical states in patients with thalamic injury. (A) Amplitude plots show the transformed raw data used for inference along with estimated 2 sigma bounds for the posterior data generating process. MCMC sample plots show binary matrices where light blue pixels indicate a sampled state transition corresponding to the upper amplitude plots. **(B)** Distributions for the number of states for patients with high/low FA values with statistically significant mean difference (p = 4e-08). **(C)** The number of states for each patient for sequential 1000 sample batches used to construct distributions in **(B)**. Here, patients are ranked based on the average FA values from whole thalamus to ACC, mPFC, and DLPFC.

easier to perform inferences on the difference of the logarithm of the raw data squared. Two examples of this transformation applied to EEG tracings from patients are shown in Fig. 3A: one with no injuries to their thalamic projections (left panel) and one with impaired thalamo-prefrontal projections (right panel). The bottom panel in Fig. 3A shows the MCMC sampling results for 5000 iterations. Each plot is a binary image where light blue indicates a sampled state transition. We can think of each row as a random draw from the posterior Yule-Simon process conditioned on the measurements for each patient as shown in the upper plot. As more MCMC steps are taken, we see the emergence of vertical lines, which indicates a high probability of state transition. This analysis revealed a statistically significant tendency (p = 4e-08) to be stuck at the visiting state for a longer period and change states less frequently for patients with low FA values as shown in Fig. 3B. As described previously, we divided the first 10,000 samples for each patient into 1000 sample batches. After applying the MCMC inference to each batch, we observed a consistent trend shown in Fig. 3C.

4. Discussion

In this manuscript, we tested our hypothesis that distributed, adaptive complex cortical dynamics associated with recovery of consciousness result from thalamic modulation of cortical connectivity. We also reported that thalamo-prefrontal connectivity is needed to recover cognitive capacity, defined by performing goal-directed behavior, after TBI (Cosgrove et al., 2022). Here, we found that the phase space of cortical dynamics in the absence of thalamo-prefrontal connections resembles a low-dimensional global attractor state with a limited and predictable trajectory of visiting states available. We confirmed these findings with multiple techniques, including RP analysis, Gaussian process prediction, and Yule-Simon analysis. In summary, impaired thalamic input is associated with constrained state dynamics, prolonged state occupancy, and high predictability. Taken together, our findings imply that the thalamus is critical to maximizing the flexibility of the cortex, which is essential for goal-directed behavior.

We propose that thalamic input controls the evolution of cortical assemblies and shapes the global landscape of cortical dynamics leading to complex EEG dynamics. When withdrawn, cortical network dynamics appear to be trapped in a global *coma attractor state*, which constrains the formation of cell assemblies needed for neuronal computations supporting goal-directed behaviors. In the context of brain injury, the global coma attractor only includes a narrow and predictable repertoire of possible states that results in a dysfunctional cortical network. Our results are in line with the new view of the thalamus: the thalamus is not a simple relay center, but it can dynamically control the distributed adaptive dynamics within and across cortical networks to support the ongoing cognitive task. Multiple reports also support this view and define a new role for the thalamus, in particular higher-order thalamic nuclei such as MD, as the regulator of cortical connectivity. Schmitt and colleagues describe the first thalamocortical model of this phenomenon in a working memory two-alternative forced choice task, where MD thalamus supports formation of neuronal ensembles responsible for maintaining the memory during the delay period (Schmitt et al., 2017). Similarly, MD has been shown to play a critical role in the selectivity of cognitive tasks as its activity sustains PFC representations during the delay period of a working memory task (Bolkan et al., 2017). Indeed,

inhibition of MD has the opposite effect and interferes with prefrontal connectivity and cognition (Parnaudeau et al., 2013). Two more recent studies suggest that MD regulates the excitatory-inhibitory balance within PFC in order to modulate its activity and connectivity (Mukherjee et al., 2020, 2021). However, future investigations will have to dissect the role of MD subpopulations expressing GRIK4 and D_2 receptors in controlling state diversity in the cortex. In agreement with these findings, a computational model of the thalamocortical system revealed that small thalamic regions can in fact control the dynamics of a large cortical area (Logiaco et al., 2021).

In the past two decades, several other studies have highlighted the role of the thalamus as the regulator of the global brain state, including awareness, attention, and cognition (Ruff, 2007; Schiff et al., 2007; Theyel et al., 2010; Kastner and Saalman, 2012; Saalmann and Kastner, 2015; Shine et al., 2019; Redinbaugh et al., 2020; Shine, 2021). Schiff and colleagues previously reported that central thalamus stimulation in a comatose TBI patient resulted in behavioral improvement (Schiff et al., 2007). Thirteen years later macaque experiments showed that thalamic firing rate was correlated with consciousness and central lateral thalamic stimulation aroused two monkeys from anesthesia (Ruff, 2007; Schiff et al., 2007; Redinbaugh et al., 2020). However, the role of other higher-order thalamic nuclei, such as the mediodorsal thalamus, in the return of goal-directed behavior following TBI is still unknown. Our data provide evidence that thalamic projections to the prefrontal cortex support the flexibility of cortical networks (Duncan, 2001) required for the return of goal-directed behavior.

An alternative possibility could be that cortical networks are independent self-organizing entities that adaptively reconfigure their connectivity independent of a remote secondary amplifier center (i.e., the thalamus). The higher-order cognitive functions required for goal-directed behavior are coded in the coordinated activity of cortical *neuronal ensembles*, an idea first introduced by Donald Hebb (2005). Wenzel and colleagues visualized formation of these ensembles in rodent and human experiments using a clustering technique ("t-Distributed Stochastic Neighbor Embedding", t-SNE) on spike-sorted Utah array data and calcium imaging of the conscious state and showed that they break down into individual cells under anesthesia (Wenzel et al., 2019). The activity of these neuronal ensembles should be cohesive to be reliably activated in response to stimuli. Their cohesiveness is due to an increased gain of synaptic connections within the ensemble compared to the rest of the network. However, hardwired connections cannot explain the flexibility and computational capacity of the brain. Previous studies have shown that a significant fraction of PFC cells can be freely recruited to the pool of cells representing the ongoing task-relevant features, which conflicts with the idea that the cortex is hardwired (Duncan, 2001; Duncan and Miller, 2002). Instead, they suggest that the effective connectivity of cortical cells can be changed adaptively depending on the current context to form or activate ad hoc neuronal ensembles needed for different tasks. Together, based on recent experimental and computational data, the involvement of thalamus as an additional layer of control, via adjusting the synaptic gain of cortical cells to activate and deactivate ensembles depending on the context seems likely.

In summary, we found that withdrawal of thalamic input results in a cortical attractor state with a limited number of states available, leading to a limited cognitive capacity. Our finding has further implications for developing future neuromodulatory approaches. Our model prediction is that augmenting the thalamic activity in patients with thalamic injury could expand the repertoire of available cortical states by facilitating the return of cortical neuronal ensembles required for cognitive functions. However, further investigations are necessary to examine this prediction.

4.1. Study limitations

Limitations of our study include the relatively small sample size and the limitation of our analysis to the thalamo-prefrontal circuit. Our sample size represents a convenience sample of severe TBI patients who underwent imaging; at present, it is very challenging to study this population because of the difficulty of obtaining imaging. Another minor issue is that two patients in the unfavorable group and one patient in the favorable group underwent procedures to remove large pieces of skull; however, these surgeries would typically increase the relative content of higher frequencies (Cobb et al., 1979; Brigo et al., 2011). We thus consider major bias from cranial surgery unlikely. Severe TBI patients are underrepresented in extensive studies such as TRACK-TBI. Thus, our study represents important pilot data for larger cohorts. We also expect that other studies will involve multiple corticothalamic circuits; this too is challenging because of the inherent difficulty of the region of interest (ROI) identification in injured brains. Future studies will use machine learning-guided ROI drawing to facilitate these analyses. Finally, we have tried to carefully specify that the return of goal-directed behavior (i.e., command following) is our proxy for consciousness throughout. Command-following is not required for consciousness, given multiple conditions that can impair this behavior, such as spinal cord injury and locked-in syndrome. Moreover, the phenomenon of "covert consciousness" appears to be widespread in ICU cohorts (Edlow et al., 2017; Claassen et al., 2019). Nonetheless, command following is a common clinical assessment method (Teasdale and Jennett, 1974) which strongly correlates with outcome (Whyte et al., 2013). In future studies, we will attempt to distinguish covert from overt command following, and the relative contributions of complex activity to each behavior.

5. Conclusion

The integrity of the thalamic projections to the prefrontal cortex supports cortical dynamics which are diverse, complex, and have low-predictability. These dynamics are important to establish a flexible repertoire of cortical states needed for the return of goal-directed behavior after TBI.

Data availability

Original recordings and images are available upon reasonable request.

Code availability

All code used in this work is available upon reasonable request.

Study funding

This work was funded by the Growing Convergence Research program (NSF Award 2021002), a FUSION-TRO award (63845) from the Renaissance School of Medicine at Stony Brook University, as well as SEED grant funding from the Office of the Vice President for Research at Stony Brook University.

Author contributions

Sima Mofakham contributed to conceptualization, data curation, formal analysis, computational modeling, investigation, methodology, validation, visualization, original draft writing, review and editing, project administration, resources, and supervision of the research. Yuhao Liu was involved with formal analysis, computation modeling, methodology, and visualization. Asher Hensley contributed to formal analysis, methodology, computational modeling, visualization, and original draft writing. Jordan R. Saadon and Theresa Gammel helped with investigation, data curation, visualization, and review and editing. Megan E. Cosgrove and Joseph Adachi performed formal analysis and data curation. Selma Mohammad was involved with formal analysis and data curation. Chuan Huang contributed to visualization, formal

analysis, and original draft writing. Petar Djurić was involved with conceptualization, methodology, resources, supervision of the research, and review and editing. Charles B. Mikell contributed to conceptualization, investigation, supervision of the research, resources, and review and editing.

Declaration of Competing Interest

The authors declare no conflict of interest.

Acknowledgments

The authors would like to thank Dr. Marc Halterman and Dr. Michael Halassa for their constructive discussion. We also thank the EEG center and the Department of Neurosurgery at Stony Brook University Hospital for supporting this research.

Appendix A. The Peer Review Overview and Supplementary data

The Peer Review Overview and Supplementary data associated with this article can be found in the online version, at doi:https://doi.org/10.1016/j.pneurobio.2022.102215.

References

Berger, H., 1929. Über das elektroenkephalogramm des menschen. Archiv für psychiatrie und nervenkrankheiten 87, 527–570.
Bolkan, S.S., Stujenske, J.M., Parnaudeau, S., Spellman, T.J., Rauffenbart, C., Abbas, A.I., Harris, A.Z., Gordon, J.A., Kellendonk, C., 2017. Thalamic projections sustain prefrontal activity during working memory maintenance. Nat. Neurosci. 20, 987–996.
Brigo, F., Cicero, R., Fiaschi, A., Bongiovanni, L.G., 2011. The breach rhythm. Clin. Neurophysiol. 122, 2116–2120.
Casali, A.G., Gosseries, O., Rosanova, M., Boly, M., Sarasso, S., Casali, K.R., Casarotto, S., Bruno, M.-A., Laureys, S., Tononi, G., Massimini, M., 2013. A theoretically based index of consciousness independent of sensory processing and behavior. Sci. Transl. Med. 5, 198ra105.
Claassen, J., Doyle, K., Matory, A., Couch, C., Burger, K.M., Velazquez, A., Okonkwo, J. U., King, J.-R., Park, S., Agarwal, S., Roh, D., Megjhani, M., Eliseyev, A., Connolly, E. S., Rohaut, B., 2019. Detection of brain activation in unresponsive patients with acute brain injury. N. Engl. J. Med. 380, 2497–2505.
Cobb, W.A., Guiloff, R.J., Cast, J., 1979. Breach rhythm: the EEG related to skull defects. Electroencephalogr. Clin. Neurophysiol. 47, 251–271.
Cosgrove, M.E., Saadon, J.R., Mikell, C.B., Stefancin, P.L., Alkadaa, L., Wang, Z., Saluja, S., Servider, J., Razzaq, B., Huang, C., Mofakham, S., 2022. Thalamo-Prefrontal Connectivity Correlates with Early Command-Following After Severe Traumatic Brain Injury. bioRxiv. https://doi.org/10.1101/2022.01.06.475131.
Djurić, P.M., Kotecha, J.H., Esteve, F., Perret, E., 2002. Sequential parameter estimation of time-varying non-gaussian autoregressive processes. EURASIP J. Adv. Signal Process. 2002, 1–11.
Domich, L., Oakson, G., Steriade, M., 1986. Thalamic burst patterns in the naturally sleeping cat: a comparison between cortically projecting and reticularis neurones. J. Physiol. 379, 429–449.
Duncan, J., 2001. An adaptive coding model of neural function in prefrontal cortex. Nat. Rev. Neurosci. 2, 820–829.
Duncan, J., Miller, E.K., 2002. Cognitive focus through adaptive neural coding in the primate prefrontal cortex. Principles Front. Lobe Funct. 63, 278–291.
Edlow, B.L., Chatelle, C., Spencer, C.A., Chu, C.J., Bodien, Y.G., O'Connor, K.L., Hirschberg, R.E., Hochberg, L.R., Giacino, J.T., Rosenthal, E.S., Wu, O., 2017. Early detection of consciousness in patients with acute severe traumatic brain injury. Brain 140, 2399–2414.
Fingelkurts, A.A., Fingelkurts, A.A., Bagnato, S., Boccagni, C., Galardi, G., 2012. EEG oscillatory states as neuro-phenomenology of consciousness as revealed from patients in vegetative and minimally conscious states. Conscious. Cogn. 21, 149–169.
Forgacs, P.B., Frey, H.-P., Velazquez, A., Thompson, S., Brodie, D., Moitra, V., Rabani, L., Park, S., Agarwal, S., Falo, M.C., Schiff, N.D., Claassen, J., 2017. Dynamic regimes of neocortical activity linked to corticothalamic integrity correlate with outcomes in acute anoxic brain injury after cardiac arrest. Ann. Clin. Transl. Neurol. 4, 119–129.
Glenn, L.L., Steriade, M., 1982. Discharge rate and excitability of cortically projecting intralaminar thalamic neurons during waking and sleep states. J. Neurosci. 2, 1387–1404.
Hebb, D.O., 2005. The Organization of Behavior: a Neuropsychological Theory. Psychology Press.
Hensley, A.A., Djurić, P.M., 2017. Nonparametric learning for Hidden Markov Models with preferential attachment dynamics. 2017 IEEE International Conference on Acoustics, Speech and Signal Processing (ICASSP) 3854–3858.
James, W., 1918. The Principles of Psychology: Authorized Ed., Unabridged. Dover Publications.
Kastner, S., Saalman, Y.B., 2012. Role of the pulvinar in regulating information transmission between cortical areas. J. Vis. 12, 1374–1374.
King, J.-R., Sitt, J.D., Faugeras, F., Rohaut, B., El Karoui, I., Cohen, L., Naccache, L., Dehaene, S., 2013. Information sharing in the brain indexes consciousness in noncommunicative patients. Curr. Biol. 23, 1914–1919.
Koch, C., Massimini, M., Boly, M., Tononi, G., 2016. Neural correlates of consciousness: progress and problems. Nat. Rev. Neurosci. 17, 307–321.
Laje, R., Buonomano, D.V., 2013. Robust timing and motor patterns by taming chaos in recurrent neural networks. Nat. Neurosci. 16, 925–933.
Leisen, F., Rossini, L., Villa, C., 2017. A note on the posterior inference for the Yule–Simon distribution. J. Stat. Comput. Simul. 87, 1179–1188.
Llinás, R.R., Steriade, M., 2006. Bursting of thalamic neurons and states of vigilance. J. Neurophysiol. 95, 3297–3308.
Logiaco, L., Abbott, L.F., Escola, S., 2021. Thalamic control of cortical dynamics in a model of flexible motor sequencing. Cell Rep. 35, 109090.
Lu, Q., Karanikolas, G., Shen, Y., Giannakis, G.B., 2020. Ensemble Gaussian processes with spectral features for online interactive learning with scalability. In: Chiappa, S., Calandra, R. (Eds.), Proceedings of the Twenty Third International Conference on Artificial Intelligence and Statistics, 108. PMLR, pp. 1910–1920.
Mofakham, S., Fry, A., Adachi, J., Stefancin, P.L., Duong, T.Q., Saadon, J.R., Winans, N. J., Sharma, H., Feng, G., Djuric, P.M., Mikell, C.B., 2021. Electrocorticography reveals thalamic control of cortical dynamics following traumatic brain injury. Commun. Biol. 4, 1210.
Mukherjee, A., Bajwa, N., Lam, N.H., Porrero, C., Clasca, F., Halassa, M.M., 2020. Variation of connectivity across exemplar sensory and associative thalamocortical loops in the mouse. Elife 9.
Mukherjee, A., Lam, N.H., Wimmer, R.D., Halassa, M.M., 2021. Thalamic circuits for independent control of prefrontal signal and noise. Nature 600, 100–104.
Parnaudeau, S., O'Neill, P.-K., Bolkan, S.S., Ward, R.D., Abbas, A.I., Roth, B.L., Balsam, P. D., Gordon, J.A., Kellendonk, C., 2013. Inhibition of mediodorsal thalamus disrupts thalamofrontal connectivity and cognition. Neuron 77, 1151–1162.
Pfurtscheller, G., Aranibar, A., 1977. Event-related cortical desynchronization detected by power measurements of scalp EEG. Electroencephalogr. Clin. Neurophysiol. 42, 817–826.
Redinbaugh, M.J., Phillips, J.M., Kambi, N.A., Mohanta, S., Andryk, S., Dooley, G.L., Afrasiabi, M., Raz, A., Saalmann, Y.B., 2020. Thalamus modulates consciousness via layer-specific control of cortex. Neuron 106, 66–75.e12.
Ruff, R., 2007. Faculty opinions recommendation of behavioural improvements with thalamic stimulation after severe traumatic brain injury. Faculty Opinions – Post-Publication Peer Review of the Biomedical Literature. https://doi.org/10.3410/f.1089473.543595.
Saalmann, Y.B., Kastner, S., 2015. The Cognitive Thalamus. Frontiers Media SA.
Schiff, N.D., Giacino, J.T., Kalmar, K., Victor, J.D., Baker, K., Gerber, M., Fritz, B., Eisenberg, B., Biondi, T., O'Connor, J., Kobylarz, E.J., Farris, S., Machado, A., McCagg, C., Plum, F., Fins, J.J., Rezai, A.R., 2007. Behavioural improvements with thalamic stimulation after severe traumatic brain injury. Nature 448, 600–603.
Schmitt, L.I., Wimmer, R.D., Nakajima, M., Happ, M., Mofakham, S., Halassa, M.M., 2017. Thalamic amplification of cortical connectivity sustains attentional control. Nature 545, 219–223.
Shine, J.M., 2021. The thalamus integrates the macrosystems of the brain to facilitate complex, adaptive brain network dynamics. Prog. Neurobiol. 199, 101951.
Shine, J.M., Hearne, L.J., Breakspear, M., Hwang, K., Müller, E.J., Sporns, O., Poldrack, R.A., Mattingley, J.B., Cocchi, L., 2019. The low-dimensional neural architecture of cognitive complexity is related to activity in medial thalamic nuclei. Neuron 104, 849–855.e3.
Sitt, J.D., King, J.-R., El Karoui, I., Rohaut, B., Faugeras, F., Gramfort, A., Cohen, L., Sigman, M., Dehaene, S., Naccache, L., 2014. Large scale screening of neural signatures of consciousness in patients in a vegetative or minimally conscious state. Brain 137, 2258–2270.
Strogatz, S.H., 2018. Nonlinear Dynamics and Chaos with Student Solutions Manual: with Applications to Physics, Biology, Chemistry, and Engineering, Second edition. CRC Press.
Synek, V.M., 1988. Prognostically important EEG coma patterns in diffuse anoxic and traumatic encephalopathies in adults. J. Clin. Neurophysiol. 5, 161–174.
Teasdale, G., Jennett, B., 1974. Assessment of coma and impaired consciousness. A practical scale. Lancet 2, 81–84.
Theyel, B.B., Llano, D.A., Sherman, S.M., 2010. The corticothalamocortical circuit drives higher-order cortex in the mouse. Nat. Neurosci. 13, 84–88.
Timofeev, I., Grenier, F., Bazhenov, M., Sejnowski, T.J., Steriade, M., 2000. Origin of slow cortical oscillations in deafferented cortical slabs. Cereb. Cortex 10, 1185–1199.
Urteaga, I., Bugallo, M.F., Djuric, P.M., 2015. Sequential Monte Carlo sampling for systems with fractional Gaussian processes. 2015 23rd European Signal Processing Conference (EUSIPCO). https://doi.org/10.1109/eusipco.2015.7362583.
Wang, Z., Winans, N.J., Zhao, Z., Cosgrove, M.E., Gammel, T., Saadon, J.R., Mani, R., Ravi, B., Fiore, S.M., Mikell, C.B., Mofakham, S., 2021. Agitation following severe traumatic brain injury is a clinical sign of recovery of consciousness. Front. Surg. 8, 627008.
Wenzel, M., Han, S., Smith, E.H., Hoel, E., Greger, B., House, P.A., Yuste, R., 2019. Reduced repertoire of cortical microstates and neuronal ensembles in medically induced loss of consciousness. Cell Syst. 8, 467–474.e4.
Whyte, J., Nakase-Richardson, R., Hammond, F.M., McNamee, S., Giacino, J.T., Kalmar, K., Greenwald, B.D., Yablon, S.A., Horn, L.J., 2013. Functional outcomes in traumatic disorders of consciousness: 5-year outcomes from the National Institute on

Disability and Rehabilitation Research Traumatic Brain Injury Model Systems. Arch. Phys. Med. Rehabil. 94, 1855–1860.
Winans, N.J., Liang, J.J., Ashcroft, B., Doyle, S., Fry, A., Fiore, S.M., Mofakham, S., Mikell, C.B., 2019. Modeling the return to consciousness after severe traumatic brain injury at a large academic level 1 trauma center. J. Neurosurg. 1–9.
Zhao, Z., Liang, J.J., Wang, Z., Winans, N.J., Morris, M., Doyle, S., Fry, A., Fiore, S.M., Mofakham, S., Mikell, C.B., 2021. Cardiac arrest after severe traumatic brain injury can be survivable with good outcomes. Trauma Surg. Acute Care Open 6, e000638.